Hindawi
Geofluids
Volume 2022, Article ID 1465777, 10 pages
https://doi.org/10.1155/2022/1465777

Research Article

Dendric Fractal Characteristics of Pores in Anthracite and Their Influences on Gas Adsorption Characteristics

Zhihui Wen,[1,2,3,4] **Bingtao Jia**,[1,3] **Jianwei Wang**,[4] **Jiangang Ren**,[5] **and Qi Wang**[1,3]

[1]*State Key Laboratory Cultivation Base for Gas Geology and Gas Control, Henan Polytechnic University, Jiaozuo, 454000 Henan, China*
[2]*Collaborative Innovation Center of Coal Work Safety and Clean High Efficiency Utilization, Jiaozuo, 454000 Henan, China*
[3]*College of Safety Science and Engineering, Henan Polytechnic University, Jiaozuo, 454000 Henan, China*
[4]*Zhengzhou Coal Industry (Group) Co. Ltd., Zhengzhou, 450000 Henan, China*
[5]*School of Resources and Environment, Henan University of Engineering, Zhengzhou 451191, China*

Correspondence should be addressed to Zhihui Wen; wenzhihui@hpu.edu.cn

Received 30 March 2022; Accepted 12 July 2022; Published 26 July 2022

Academic Editor: Basim Abu-Jdayil

The characteristics of pores in anthracite from Guhanshan Coal Mine in the Jiaozuo mining area were tested by the mercury injection method. According to the pore size, pores in the coal sample were classified into gas seepage pores and gas adsorption pores which were in line with the stochastic fractal model and the dendric fractal model, respectively. Besides, the fractal characteristics of adsorption pores were analyzed by using a dendric fractal model, and the influence law of the tortuosity fractal dimension D_t on the gas adsorption capacity was obtained. The research results show that the amount of mercury injected into each experimental coal sample is directly proportional to its porosity, but has no obvious correlation with specific surface area. Seepage pores with sizes over 65 nm fit the stochastic fractal model, and their fractal dimension D increases with the increase of specific surface area. Adsorption pores with sizes of below 65 nm fit the dendric fractal model, and their tortuosity fractal dimension D_t is positively correlated with the specific surface area. Through the gas adsorption experiment on coal samples, it is found that a larger D_t corresponds to a stronger gas adsorption capacity. The research results can provide a theoretical basis for elucidating the gas adsorption characteristics of anthracite from a microscopic point of view.

1. Introduction

China is a country that is rich in coal resources and lacks oil and gas resources. Such resource characteristics guarantee coal's strategic position and its role as a basic energy will maintain for a long time [1, 2]. However, as coal mining develops into the deep, recurrent gas outburst accidents make gas prevention and control work top priorities [3, 4]. Coal, as a typical heterogeneous porous medium, has a pore structure whose characteristics determine the occurrence and flow law of internal gas, and its adsorption capacity for gas is closely related to the pore structure [5–8]. Therefore, research on the pore structure of coal is of great significance for clarifying the regularity of gas occurrence and migration in coal.

The fractal geometry theory founded by French mathematician Mandelbrot [9] provides a new idea for investigating the complex microscopic pore structure of porous medium. Chen et al., Chen et al., Wei et al., and He et al. [10–13] have carried out relevant researches on the fractal characteristics of coal pore structure and concluded that coal surface has significant fractal characteristics. Liu et al. [14] discussed the pore structure characteristics and fractal characteristics of different rank coals by low temperature liquid nitrogen adsorption method and believed that the fractal dimension D could quantitatively characterize the roughness of coal surface, and its value increased with the increase of coal rank. In a study of Li et al. [15], the pore structure and coal composition during different coalification stages have specific effects on the fractal characteristics of pore shape, surface, and volume. In a study of Si et al. [16], the variation rule of the coal pore structure before and after water leaching and its influences on gas adsorption

characteristics were tested through low-temperature N_2 and CO_2 adsorption experiments. Wang et al. [17] examine the changes in pore structures of different coal samples using liquid nitrogen adsorption, nuclear magnetic resonance, and X-ray photoelectron spectroscopy. Wang et al. [18, 19] scanned coal samples based on the industrial CT scanning experimental system, and analyzed the relation between the fractal dimension and the development degree of the fracture structure inside coal samples. Ma et al. and Cai et al. [20, 21] discussed the fractal characteristics of the coal pore structure and its influences on permeability. In the studies of Nie et al. [22–24], the diffusion coefficient and the permeability were calculated by using fractal characteristics of the pore structure, and a relation between the adsorption characteristics of coal samples and the fractal dimension on the pore surface was established through a cryogenic nitrogen adsorption experiment. Adopting a stochastic fractal model to describe the fractal of pores of the coal body, Li et al. [25] stated that only when P is below 10 MPa, the pores measured by the mercury injection method have the characteristics of the stochastic fractal model, and the corresponding pore radius is about 60 nm. Jia et al. [26] analyzed Yangquan anthracite samples by liquid nitrogen adsorption and found that the specific surface area of anthracite micropores and mesopores increased with decreasing particle size. Lu et al. [27] found that the overall pore volume and specific surface of anthracite coal were positively correlated with the fractal size of the pore structure by fractal calculations of the nitrogen adsorption capacity of the coal.

Gas occurrence and migration are related not only to pore volume but also to pore length and number. On this basis, Wheatcraft and Tyler [28] established the Lagrangian model to depict the relation between pore length and pore size. In the studies of Yu and Cheng and Xu et al. [29, 30], a dendric fractal model of the pore structure of a porous medium was established by combining the Lagrangian model and the law of power that describes the number of pores. This model considers the fractal characteristics of the number, length, and pore size of the porous medium and is applied to research the relation between the fractal dimension and the permeability and diffusion coefficient of the porous medium.

At present, the fractal characteristics of coal rock adsorption pores are rarely studied by using the dendric fractal model to analyze mercury injection experimental results. In this paper, relevant experiments were performed on the pore distribution characteristics of anthracite from Guhanshan Coal Mine in the Jiaozuo mining area, China. The pores of coal samples were classified into two categories, i.e., gas seepage pores and gas adsorption pores, according to pore size. The fractal characteristics of seepage pores were analyzed by using the stochastic fractal model, while those of adsorption pores by using the dendric fractal model. Besides, the relation between the tortuosity fractal dimension of the dendric fractal model and the gas adsorption capacity of the coal body was studied through a gas adsorption experiment. The results provide a theoretical basis for elucidating the gas adsorption characteristics of anthracite from a microscopic point of view.

2. Pore Fractal Model

The coal rock porous medium is composed of particles of different sizes, which is quite similar to the construction process of fractal. Hence, the fractal model can be used for quantitative analysis. In a self-similarity system, after i times of iterations, the relation between the number and the size of units can be illustrated by the following equation [25]:

$$N\left(\frac{1}{b^i}\right) = K\left(\frac{1}{b^i}\right)^{-D} (i = 0, 1, 2, \cdots), \tag{1}$$

where $N(1/b^i)$ is the number of units whose length is $1/b^i$; K is the number of initial elements per unit length; i is the number of iterations; b is the size-transformation factor, with its value over 1; D is the fractal dimension. Equation (1) is a general equation of the fractal construction, independent of the dimension and the construction method of initial elements.

2.1. Stochastic Fractal Model. The mercury injection experiment is a commonly used method to test characteristics of pores in coal samples. In order to overcome the inner surface pressure between mercury and pore surface, the pressure P required to inject mercury into pores and the pore radius r satisfy the Washburn equation [28]:

$$P = (-2\sigma \cos a)/r, \tag{2}$$

where P is the mercury injection pressure, MPa; a is the wetting contact angle of mercury, 140°; σ is the surface tension of mercury, 10^{-3} N/m; r is the pore radius, nm.

During the experiment, the mercury injection volume V_p is equal to the sum of the volume of pores whose sizes are over r, under a given pressure condition. The porous medium dV_p/dr constructed by Mengar and the fractal dimension D satisfy the following equation:

$$\frac{dV_p}{dr} \propto r^{2-D}. \tag{3}$$

Equation (4) can be obtained by substituting Eq. (2) into Eq. (3):

$$\frac{dV_p}{dP} \propto P^{D-4}. \tag{4}$$

Equation (5) can be obtained by taking the logarithm of both ends of Eq. (4):

$$\lg \frac{dV_p}{dP} \propto (D-4) \lg P, \tag{5}$$

where V_p is the pore volume, cm^3/g; D is the fractal dimension of coal rock.

According to Eq. (5), if pore distribution conforms to fractal characteristics, a linear relation exists between $\lg(dV_p/dP)$ and lgP, and the coal fractal dimension D can be

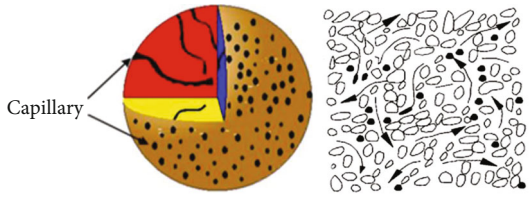

Figure 1: A capillary spherical model of coal particle.

Figure 2: Auto pore 9505 automatic mercury porosimeter.

expressed as

$$D = k + 4. \tag{6}$$

In Eq. (6), k is the slope of the fitting line between $\lg(dV_p/dP)$ and lgP.

2.2. Dendritic Fractal Model. The process of gas adsorption and diffusion in a porous medium is rather complex. In this paper, pores of coal particles are regarded as capillaries with certain tortuosity, complying with fractal characteristics [31]. The length of a capillary is much longer than the radius, and the flow of gas in the capillary is one-dimensional. The capillary spherical model [32] is shown in Figure 1.

Yu and Cheng [29] argued that the size distribution and structure of pores in a porous medium satisfy the fractal characteristics, and the cumulative pore number distribution function meets:

$$N(\geq d) = \left(\frac{d_{\max}}{d}\right)^{D_f}, \tag{7}$$

where d (nm) is the pore diameter; N is the number of pores with a diameter of over or equal to d; $d_{\max}$ (μm) is the maximum pore diameter; D_f is the fractal dimension of pores calculated by the dendritic model, and the values in two and three dimensions are $0 < D_f < 2$ and $0 < D_f < 3$, respectively.

Equation (7) is regarded as a continuous differentiable function, and the number of pores whose diameters range from d to $d + dd$ could be obtained by taking the derivative of the pore size d through Eq. (7):

$$-dN = D_f d_{\max}^{D_f} d^{-D_f-1} dd. \tag{8}$$

In Eq. (8), $-dN > 0$ indicates that the number of pores is negatively correlated with the pore radius.

Meanwhile, according to the dendric fractal model and law, the pore length L satisfies

$$L = d^{1-D_t} {L_0}^{D_t}, \tag{9}$$

where L (nm) is the pore length; L_0 (nm) is the straight-line distance of gas flow direction; D_t is the fractal dimension of pore tortuosity.

In the mercury injection experiment, the pore diameter corresponding to the ith mercury injection pressure point is d_i; that corresponding to the d_{i+1} mercury injection pressure point is $d_{i+1} = d_i + dd$; the mercury injection amount from the ith to the $i + 1$th mercury injection pressure point is dV_p. Then, the pore volume V_p of pores with a diameter of d_i to $d_i + dd$ satisfies

$$dV_p = \frac{\pi d^2}{4} LdN. \tag{10}$$

Equation (11) can be obtained by substituting Eqs. (8) and (9) into Eq. (10):

$$-\frac{dV_p}{dd} = \frac{\pi}{4} {L_0}^{D_t} D_f d_{\max}^{D_f} d^{2-D_t-D_f}. \tag{11}$$

Taking the logarithm of both ends of Eq. (11) leads to

$$\lg\left(-\frac{dV_p}{dd}\right) = (2 - D_t - D_f)\lg d + \lg\left(\frac{\pi}{4} {L_0}^{D_t} D_f \lambda_{\max}^{D_f}\right), \tag{12}$$

where L and $d_{\max}$ are known quantities, and the fractal dimension of coal rock pores can be determined through the straight line between $\lg(dV_P/dd)$ and lgd. According to Eq. (12), if pore distribution conforms to the fractal characteristics, $\lg(dV_p/dd)$ and lgd have a linear relation, and the slope k and the intercept b satisfy

$$2 - D_t - D_f = K, \tag{13}$$

$$\lg\left(\frac{\pi}{4} {L_0}^{D_t} D_f d_{\max}^{D_f}\right) = b. \tag{14}$$

3. Experiments and Results

3.1. Mercury Injection Experiment. The anthracite in the experiment was taken from Guhanshan Coal Mine in the Jiaozuo mining area. The screened coal samples with particulate sizes of 5-6 mm were divided into 4 groups and numbered from GHS-W1 to GHS-W4, respectively. The pore distribution test on coal samples was completed in the

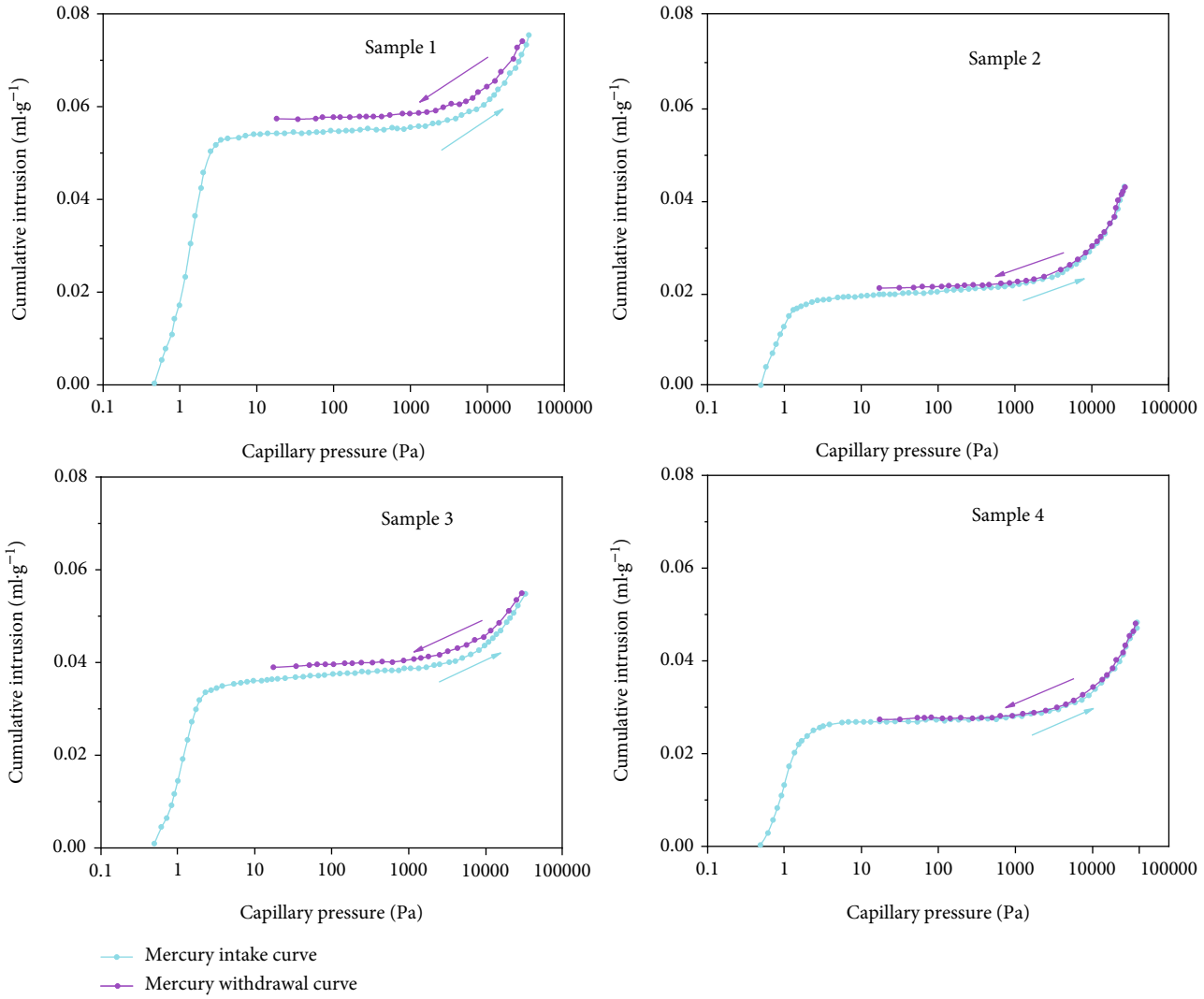

Figure 3: Mercury intake-withdrawal curves of coal samples under different pressures.

Table 1: Pore parameters of coal samples.

Coal sample	Porosity %	Specific surface area m^2/g	Total mercury injection volume ml/g
GHS-W1	10.0179	7.144	0.0754
GHS-W2	5.8580	7.519	0.0421
GHS-W3	7.6209	5.932	0.0544
GHS-W4	6.2900	6.933	0.0483

mercury injection laboratory of Safety College of Henan Polytechnic University. The experimental instrument, auto pore 9505 automatic mercury injection instrument with a mercury injection pressure of 0.03-227.5 MPa, was produced by Micromeritics Company of the United States (Figure 2).

Mercury was injected into pores of coal samples by applying external force. The applied external force and the pore radius meet Eq. (2). The pore specific surface area of samples can be further calculated according to the mercury injection pressure. It is obtained from the Young-Duper equation:

$$-PdV_P = \sigma \cos adS, \tag{15}$$

where S (m^2/g) is the specific surface area of pores.

3.2. Experimental Results. The mercury intake-withdrawal curves of GHS-W1, GHS-W2, GHS-W3, and GHS-W4 samples were obtained in the experiment (Figure 3).

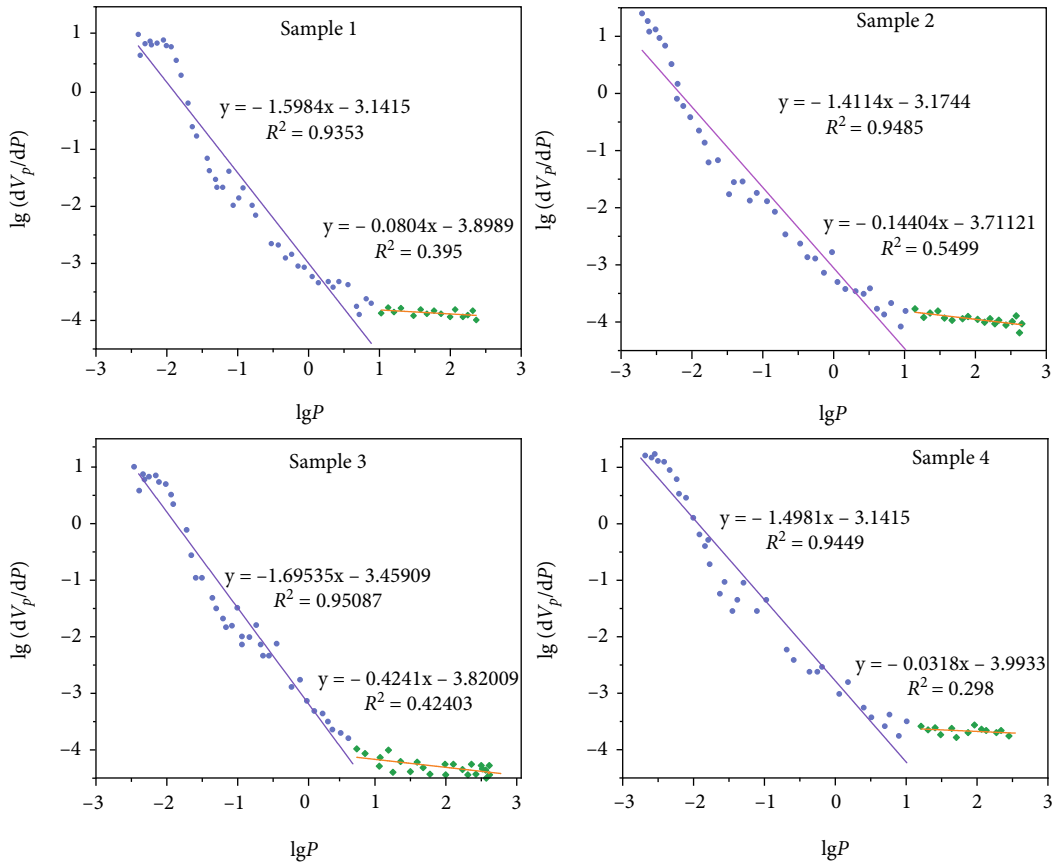

Figure 4: Fitting curves of mercury injection experimental data.

Table 2: Fractal dimensions of the stochastic fractal model.

Coal sample	Porosity %	Specific surface area m^2/g	Fractal dimension D	
			Adsorbed pore	Seepage pore
GHS-W1	10.0179	7.144	2.4016	3.9196
GHS-W2	5.8580	7.519	2.5886	3.8559
GHS-W3	7.6209	5.932	2.3047	3.5759
GHS-W4	6.2900	6.933	2.5019	3.9682

It can be seen from Figure 3 that with the increase of pressure, the mercury intake-withdrawal curves rise first and then gradually coincide, indicating that the methane adsorption mechanisms of coal differ in different pressure stages. Such a difference is mainly affected by the microscopic pore structure of coal particles. Therefore, the analysis of the microscopic pore structure of coal using the fractal theory conduces to further exploring the methane adsorption characteristics of coal. The mercury injection amount and the pore parameters of each coal sample obtained are listed in Table 1.

As can be observed from Table 1, in descending order, the mercury injection amounts follow GHS-W1, GHS-W3, GHS-W4, and GHS-W2; the porosities follow GHS-W1, GHS-W3, GHS-W4, and GHS-W2 as well; the specific surface areas follow GHS-W2, GHS-W1, GHS-W4, and GHS-W3. The above data suggest that the total mercury injection amount in the experiment is positively correlated with the porosity of coal, but has no clear correlation with the specific surface area. This is mainly because the mercury is injected into pores of coal samples by applying external force in the mercury injection experiment. A larger pore volume corresponds to more injected mercury. The pore volume is directly proportional to porosity, but is not correlated with specific surface area.

4. Analysis and Discussion

4.1. Fractal Dimensions of Gas Seepage Pores. According to the method described in Section 2.1, $\lg(dV_p/dP)$ and lgP were calculated by using the stochastic fractal model. In the rectangular coordinate system, with lgP as the abscissa and $\lg(dV_p/dP)$ as the ordinate, a scatter diagram was plotted and a linear fitting was carried out. The results are displayed in Figure 4.

As can be seen from Figure 4, when P is below 10 MPa (pore radius > 65 nm), $\lg(dV_p/dP)$ is linearly correlated with lgP obviously, and the curve fitting degree is over 0.93. However, when P is above 10 MPa (pore radius < 65 nm), the linear fitting degree is below 0.6. It is a proof that the stochastic fractal model is only applicable to seepage pores whose pore radius is over 65 nm, but cannot depict adsorption pores with a pore radius of below 65 nm. The fractal dimensions of coal samples are calculated according to the slope of the fitting line (Table 2).

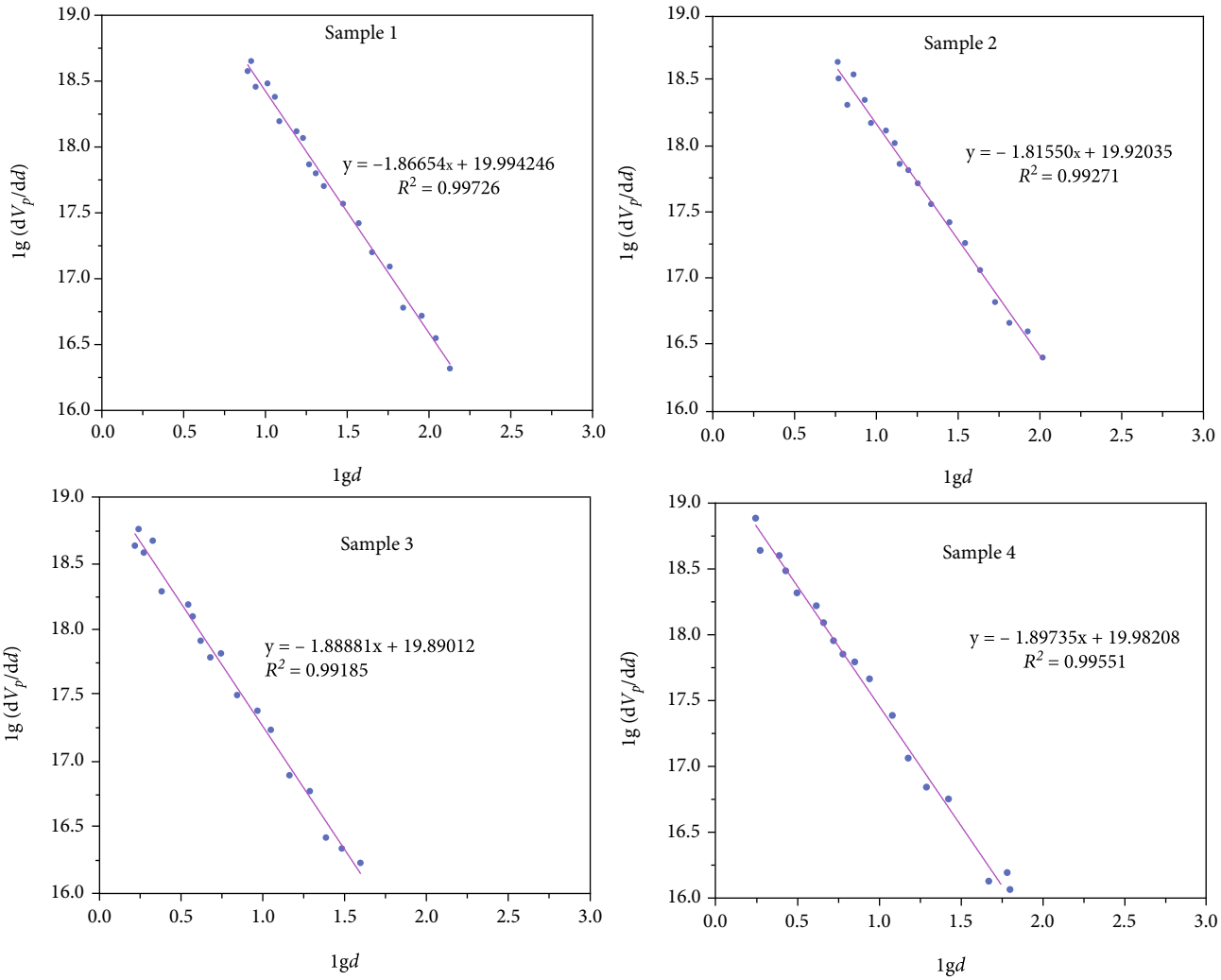

Figure 5: Fitting curves of $\lg(dV_P/dd)$ and lgd.

Table 3: Fractal dimensions of the tree fractal model.

Coal sample	Porosity %	Specific surface area m^2/g	D_f	D_t
GHS-W1	10.0179	7.144	1.48654	2.38000
GHS-W2	5.8580	7.519	1.38936	2.42614
GHS-W3	7.6209	5.932	1.54814	2.34067
GHS-W4	6.2900	6.933	1.53667	2.36068

According to Table 2, when the pressure P is below 10 MPa, fractal dimensions of coal samples lie in the range of 2-3; when it is over 10 MPa, those are over 3. From the perspective of classical geometry, $2 < D < 3$ in a three-dimensional space, that is, $D > 3$ is meaningless, which is consistent with the research results of Li et al. [25]. This further suggests that the use of the stochastic fractal model to analyze mercury injection experimental results is only applicable to gas seepage pores whose radii are over 65 nm.

4.2. Fractal Dimensions of Gas Adsorption Pores. According to the method described in Section 2.2, $\lg(dV_P/dd)$ and lgd were calculated by using the dendric fractal model. In the rectangular coordinate system, with lgd as the abscissa and $\lg(dV_P/dd)$ as the ordinate, a scatter diagram was plotted, and linear fitting was carried out. The tortuosity fractal dimension was calculated by combining Eqs. (13) and (14) (Figure 5).

As shown in Figure 5, a good linear relation exists between $\lg(dV_P/dd)$ and lgd, and the fitting degree of the curve is over 0.99, that is, adsorption pores with the sizes of below 65 nm conform to the dendric fractal model.

The slope k and intercept b of the line could be obtained by linearly fitting the relation between $\lg(dV_P/dd)$ and lgd. The pore characteristic length and the maximum pore diameter were taken as $L_0 = 3$ mm and $d_{max} = 10\ \mu$m, respectively [33]. The fractal dimensions D_t and D_f of GHS-W1—GHS-W4 could be obtained from Eqs. (13) and (14), and the results are presented in Table 3.

As can be observed from Table 3, the tortuosity fractal dimension D_t increases as the specific surface area increases,

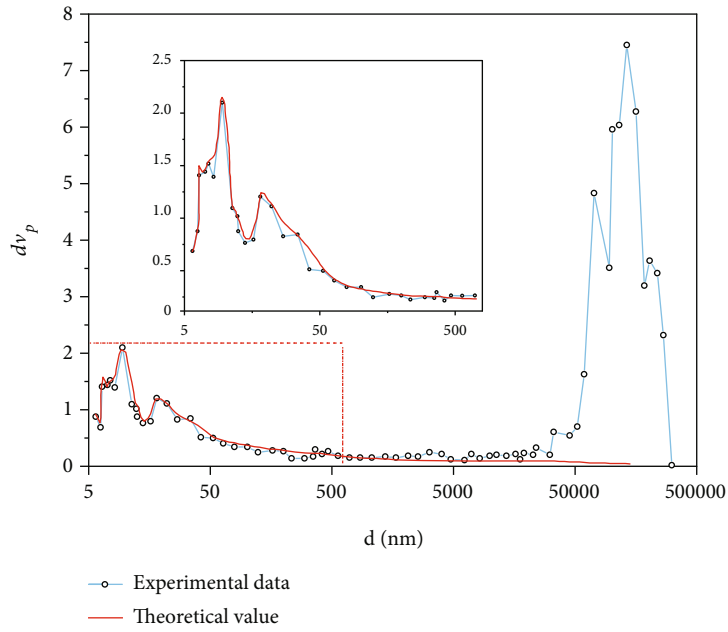

Figure 6: Relation between pore volume dV_p and diameter d.

and they show a positive correlation. However, the porosity does not have direct relations to the fractal dimensions D_f and D_t. This is because the porosity is mainly determined by mesopores and macropores whose sizes are over 100 nm, while the fractal dimensions D_f and D_t mainly describe the fractal characteristics of adsorption pores whose sizes are below 65 nm.

4.3. Relation between Pore Volume dV_p and Pore Size d. In order to facilitate the comparison with experimental results, the pore size corresponding to each pressure point in the mercury injection experiment was taken as the pore size d, and the fractal dimension D_f of adsorption pores was put into Eq. (7) to obtain the amounts (N_i and N_{i+1}) of pores whose diameters are over d_i and d_{i+1}. Afterwards, dN was obtained by a subtraction of N_i from N_{i+1}. The fractal dimension D_t of adsorption pores was substituted into Eq. (9) to obtain the diameter d and the corresponding pore length L. By substituting dN and L into Eq. (10), the curve of pore volume dV_p variation with the diameter d could be obtained. The curves of the pore volume dV_p of adsorption and seepage pores of GHS-W1 variation are with the diameter d, and their experimental and theoretical values are compared (Figure 6).

According to the curve of GHS-W1 pore volume dV_p variation with the diameter d in Figure 6, the theoretical value of dendric fractal highly matches the experimental results when the pore size is below 1 μm. When the pore size is over 1 μm, the experimental value is greater than the theoretical value, because a certain number of cracks exist in coal rock. These cracks are regarded as pores during the mercury injection experiment. Therefore, as mercury is injected into the cracks rapidly at the beginning of the experiment, the amount of mercury during this time should be subtracted to calculate the real porosity of coal rock pores. Furthermore, according to the dV_p variation curve of GHS-W1 (pore sizes 5-500 nm) with the diameter d, the dendric theoretical value of adsorption pores is in good agreement with the experimental results, with a fitting degree of 0.991, which is consistent with the conclusion that the pore specific surface area of coal samples is positively correlated with the tortuality fractal dimension D_t in Section 3.2. It is a mark that the distribution of adsorption pores of coal rock conforms to the dendric fractal model.

5. Influences of the Tortuality Fractal Dimension D_t on Gas Adsorption Characteristics

The specific surface area of coal determines the gas adsorption capacity of coal. When the specific surface area is larger, more adsorption sites are provided by coal, and more gas can be absorbed by coal. The number of micropores makes a decisive contribution to the specific surface area of pores. Hence, the influences of the tortuality fractal dimension D_t on gas adsorption characteristics can be explored through the gas adsorption experiment on coal samples.

Since the specific surface area of coal is positively correlated with the tortuosity fractal dimension D_t, it can be inferred that V_L is also positively correlated with D_t. Therefore, the authors verified the above prediction through a gas adsorption experiment on coal samples.

5.1. Gas Adsorption Experimental Results. In order to analyze the difference of the gas adsorption capacities of the four groups of coal samples, the selected coal samples were tested

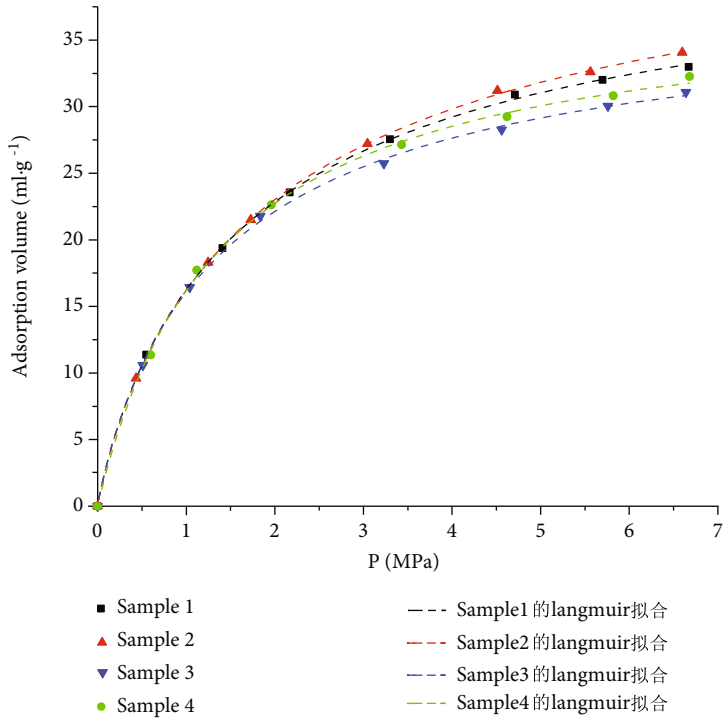

Figure 7: Gas adsorption experiment results and fitting curve.

Table 4: Gas adsorption experimental results.

Coal sample	V_L ml/g	P_L MPa	Correlation coefficient R^2
GHS-W1	33.106	0.9672	0.995
GHS-W2	34.221	0.9159	0.992
GHS-W3	30.824	1.1107	0.990
GHS-W4	31.821	1.0561	0.993

according to the "Determination Method of methane adsorption capacity of Coal (High Pressure Capacity Method)" (MT/T752-1997), and the gas adsorption capacity of coal samples at each adsorption equilibrium point was calculated.

At present, the Langmuir equation $V = V_L P/(P + P_L)$ is the most commonly used method to describe gas adsorption characteristics of coal. In the equation, V_L (ml/g) is the Langmuir volume, representing the maximum adsorption capacity of single molecular layer; P_L (MPa) is the Langmuir pressure, representing the pressure when the adsorption amount reaches half of V_L. The results of the gas adsorption experiment on each coal sample were fitted and calculated according to the Langmuir equation for the purpose of obtaining relevant adsorption characteristic parameters (Figure 7 and Table 4).

It can be observed from Figure 7 and Table 4 that the fitting degrees of gas adsorption experiment results of all coal samples are all over 0.99 according to the Langmuir equation, and the gas adsorption characteristic curves of all coal samples conform to the Langmuir equation. The Langmuir pressures P_L of the four groups of coal samples follow the order $W2 < W1 < W4 < W3$; the limit gas adsorption capacities V_L follow the order $W3 < W4 < W1 < W2$. Meanwhile, when the pressure is low (below 2 MPa), the gas adsorption capacities of the four groups of coal samples differ insignificantly. With the further increase of the pressure, a significant difference appears in the gas adsorption capacity, which is mainly caused by the difference in the internal pore microstructure.

5.2. Influences of the Tortuosity Fractal Dimension D_t on Gas Adsorption. In order to figure out the relations between the dendric tortuality fractal dimension D_t and the Langmuir volume V_L and Langmuir pressure P_L, the gas adsorption characteristic parameters of the four groups of coal samples were fitted with D_t, and the results are exhibited in Figure 8.

It can be found from Figure 8 that the dendric tortuality fractal dimension D_t of experimental coal samples is positively correlated with V_L and negatively correlated with P_L, which is attributed to the fact that the dendric tortuality fractal dimension D_t characterizes the complexity of pores of coal samples. To be specific, it depicts the bending effect of pores rather than the size of pores, reflecting the roughness of pore surface and the difficulty of the flow through the solid phase. Generally, a larger D_t corresponds to a coarser coal pore surface, a more complex pore structure, and a larger specific surface area of the corresponding coal sample, and thus more points available for gas adsorption, which is manifested by the larger V_L of the coal sample.

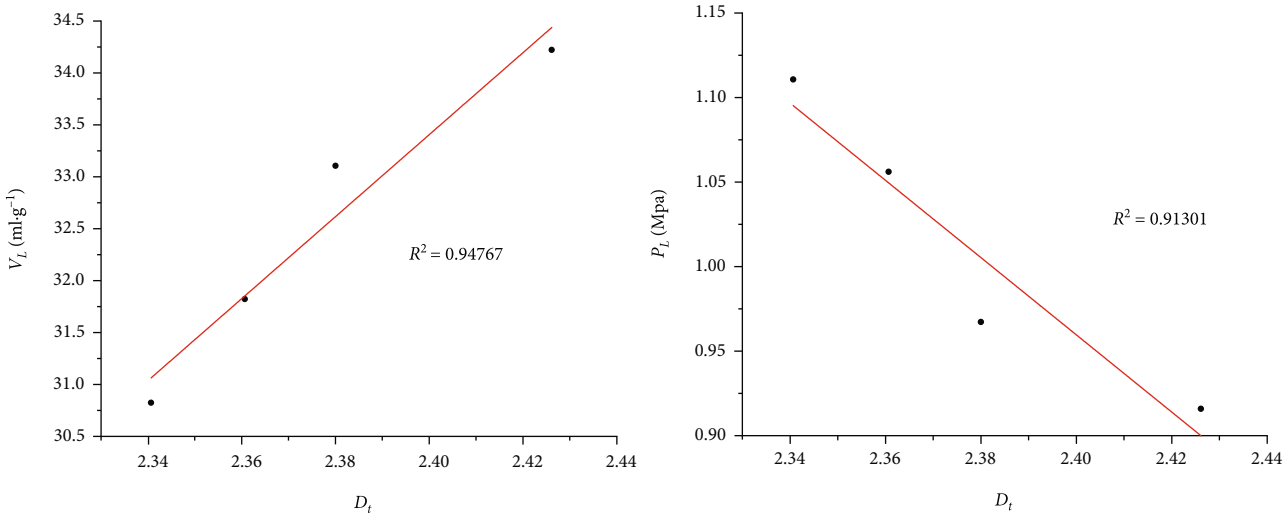

Figure 8: D_t effects on gas adsorption.

Meanwhile, the stronger the gas adsorption capacity of the coal sample is, the smaller the energy required to absorb a certain amount of gas is, which is manifested as a larger tortuality fractal dimension D_t corresponding to a smaller P_L.

6. Conclusions

Though the mercury injection experiment and the gas adsorption experiment on anthracite from Guhanshan Coal Mine in the Jiaozuo mining area, the pore dendric fractal characteristics of anthracite and their influences on gas adsorption characteristics are discussed in this paper. The following conclusions were drawn through research and analysis:

(1) The total mercury injection amount of anthracite is directly proportional to the porosity, but bears no obvious correlation with the specific surface area

(2) The mercury injection experiment on anthracite reveals that seepage pores whose sizes are over 65 nm conform to the stochastic fractal model, and the fractal dimension D increases with the increase of specific surface area; adsorption pores whose sizes are below 65 nm conform to the dendric fractal model, and the tortuosity fractal dimension D_t is positively correlated with the specific surface area of coal

(3) According to the gas adsorption experiment on various coal samples, the gas adsorption characteristic curves of anthracite all agree with the Langmuir equation, and the Langmuir pressures P_L of the four groups of coal samples follow the order $W2 < W1 < W4 < W3$; the limit gas adsorption capacities V_L follow the order $W3 < W4 < W1 < W2$

(4) The dendric tortuosity fractal dimension D_t of anthracite is positively correlated with V_L and negatively correlated with P_L. The reason is that the tortuosity fractal dimension D_t characterizes the complexity of internal pores. To be specific, it depicts the bending effect of pores rather than the size of pores, reflecting the roughness of the pore surface and the difficulty of the flow through the solid phase

Data Availability

The data used to support the findings of this study are included within the article.

Conflicts of Interest

The authors declare that they have no conflicts of interest.

Acknowledgments

This work was supported by the Project funded by China Postdoctoral Science Foundation (Grant no.: 2021M700132), the Fundamental Research Funds for the Universities of Henan Province (Grant no.: NSFRF210301), and the Doctoral Fund of Henan Polytechnic University (Grant no.: B2019-55).

References

[1] H. P. Xie, L. X. Wu, and D. Z. Zheng, "Prediction on the energy consumption and coal demand of China in 2025," *Journal of China Coal Society*, vol. 44, no. 7, pp. 1949–1960, 2019.

[2] L. Yuan, N. Zhang, J. G. Han, and Y. Wang, "The concept, model and reserve forecast of green coal resources in China," *Journal of China University of Mining & Technology*, vol. 47, no. 1, pp. 1–8, 2018.

[3] Z. H. Wen, Y. W. Yuan, J. P. Wei, J. W. Wang, L. L. Si, and Y. P. Yang, "Study on gas production mechanism of medium- and low-rank coals excited by the external DC electric field," *Fuel*, vol. 324, article 124704, 2022.

[4] X. S. Zhao, J. Cao, B. Wang, and X. L. Yang, "Experiment study of outburst pulverized coal-gas two-phase flow and

characteristic analysis of outburst wave," *Geofluids*, vol. 2021, Article ID 8186230, 11 pages, 2021.

[5] L. L. Si, H. T. Zhang, J. P. Wei, B. Li, and H. K. Han, "Modeling and experiment for effective diffusion coefficient of gas in water- saturated coal," *Fuel*, vol. 284, article 118887, 2021.

[6] D. Ma, H. Y. Duan, Q. Zhang et al., "A numerical gas fracturing model of coupled thermal, flowing and mechanical effects," *CMC-Computers Materials & Continua*, vol. 65, no. 3, pp. 2123–2141, 2020.

[7] J. H. Fu, X. L. Li, and Z. M. Wang, "A novel sealing material and a bag-grouting sealing method for underground CBM drainage in China," *Construction and Building Materials*, vol. 299, article 124016, 2021.

[8] Z. H. Wen, Q. Wang, Y. P. Yang, and L. L. Si, "Pore structure characteristics and evolution law of different-rank coal samples," *Geofluids*, vol. 2021, Article ID 1505306, 17 pages, 2021.

[9] B. B. Mandelbrot, "The fractal geometry of nature," *American Journal of Physics*, vol. 51, no. 3, p. 286, 1983.

[10] L. Y. Chen, X. J. Li, Z. H. Shen, J. Bi, Y. Liu, and S. Q. Xu, "Pore structure and fractal characteristics of outburst coal in northern Guizhou," *China Safety Science Journal*, vol. 30, no. 2, pp. 66–72, 2020.

[11] X. J. Chen, S. Zhao, Z. X. Si, L. L. Qi, and N. N. Kang, "Fractal characteristics of pore structure of coal with different metamorphic degrees and its effect on gas adsorption characteristics," *Coal Science and Technology*, vol. 48, no. 2, pp. 118–124, 2020.

[12] J. P. Wei, S. H. Dai, Z. H. Wen, X. C. Ren, and M. G. Li, "Research on comprehensive characterization method of different rank coal porosity," *Journal of Henan Polytechnic University(Natural Science)*, vol. 34, no. 3, pp. 305–310, 2015.

[13] S. S. He, D. F. Zhao, J. Liu, and W. Zhang, "Characterization of adsorption pore structure and fractal characteristics in anthracite coal based on low temperature nitrogen adsorption," *Coal Technology*, vol. 38, no. 1, pp. 66–69, 2019.

[14] Y. W. Liu, X. M. Zhang, and J. Miao, "Study on evolution of pore structure of medium and high rank coals," *Safety in Coal Mines*, vol. 51, no. 11, pp. 7–13, 2020.

[15] Z. T. Li, D. M. Liu, Y. D. Cai, Y. P. Wang, and J. Teng, "Adsorption pore structure and its fractal characteristics of coals by N_2 adsorption/desorption and FESEM image analyses," *Fuel*, vol. 257, article 116031, 2019.

[16] L. L. Si, Y. J. Xi, H. Y. Wang, Z. H. Wen, and J. P. Wei, "The characteristics of pore structure and gas adsorption for water-immersion coal after drying," *Coal Geology & Exploration*, vol. 49, no. 1, pp. 100–107, 2021.

[17] Z. J. Wang, X. L. Li, X. Gao, D. Y. Chen, and Z. G. Zhu, "Experimental research on the influence of microwave radiation on coal permeability and microstructure," *ACS Omega*, vol. 6, no. 50, pp. 34375–34385, 2021.

[18] D. K. Wang, Q. Wei, J. P. Wei, X. Bai, C. Yu, and P. Zhang, "Fractal characteristics of fracture structure and fractal seepage model of coal," *Journal of China University of Mining & Technology*, vol. 49, no. 1, pp. 103–109, 2020.

[19] D. K. Wang, F. C. Zeng, J. G. Wang et al., "Dynamic evolution characteristics and fractal law of loaded coal fractures by micro industrial CT," *Chinese Journal of Rock Mechanics and Engineering*, vol. 39, no. 6, pp. 1165–1174, 2020.

[20] D. Ma, H. Y. Duan, and J. X. Zhang, "Solid grain migration on hydraulic properties of fault rocks in underground mining tunnel: radial seepage experiments and verification of permeability prediction," *Tunnelling and Underground Space Technology*, vol. 126, article 104525, 2022.

[21] Y. D. Cai, D. M. Liu, Y. B. Yao, J. Q. Li, and J. L. Liu, "Fractal characteristics of coal pores based on classic geometry and thermodynamics models," *Acta Geologica Sinica-English Edition*, vol. 85, no. 5, pp. 1150–1162, 2011.

[22] B. S. Nie, X. F. Liu, L. L. Yang, J. Q. Meng, and X. C. Li, "Pore structure characterization of different rank coals using gas adsorption and scanning electron microscopy," *Fuel*, vol. 158, pp. 908–917, 2015.

[23] B. S. Nie, J. B. Zhang, X. F. Liu, S. Liu, and J. Q. Meng, "Research on nanopore characteristics and gas diffusion in coal seam," *Journal of Nanoscience and Nanotechnology*, vol. 17, no. 9, pp. 6765–6770, 2017.

[24] B. S. Nie, K. D. Wang, Q. Gao, and M. W. Cao, "Pore distribution and variation rules of the coal sample with CO2 adsorption at different pressures based on small-angle X-ray scattering," *Energy & Fuels*, vol. 35, no. 3, pp. 2243–2252, 2021.

[25] Z. W. Li, B. Q. Lin, Z. Y. Hao, Y. B. Gao, and F. F. Liu, "Fractal characteristics of porosity for porous media in coal mass," *Journal of Mining & Safety Engineering*, vol. 30, no. 3, pp. 437–442, 2013.

[26] H. J. Jia, Y. C. Jin, and Y. Sun, "Experimental study on pore structure of different size coal of Yangquan anthracite," *China Sciencepaper*, vol. 14, no. 10, pp. 1050–1054, 2019.

[27] W. Lu, Z. D. Zhuang, W. R. Zhang et al., "Study on the pore and crack change characteristics of bituminous coal and anthracite after different temperature gradient baking," *Energy & Fuels*, vol. 35, no. 23, pp. 19448–19463, 2021.

[28] S. W. Wheatcraft and S. W. Tyler, "An explanation of scale-dependent dispersivity in heterogeneous aquifers using concepts of fractal geometry," *Water Resources Research*, vol. 24, no. 4, pp. 566–578, 1988.

[29] B. M. Yu and P. Cheng, "A fractal permeability model for bi-dispersed porous media," *International Journal of Heat and Mass Transfer*, vol. 45, no. 14, pp. 2983–2993, 2002.

[30] P. Xu, B. M. Yu, S. X. Qiu, and J. C. Cai, "An analysis of the radial flow in the heterogeneous porous media based on fractal and constructal tree networks," *Physica A: Statistical Mechanics and its Applications*, vol. 387, no. 26, pp. 6471–6483, 2008.

[31] D. J. Xue, A. B. Zhao, K. C. Liu et al., "On the theoretical calculation of tortuosity in porous media and its experimental validation," *Journal of Mining Science and Technology*, vol. 6, no. 5, pp. 615–622, 2021.

[32] Z. H. Wen, Q. Wang, J. G. Ren, L. L. Zhang, and Y. W. Yuan, "Dynamic gas diffusion model of capillary pores in a coal particle based on pore fractal characteristics," *Transport in Porous Media*, vol. 140, no. 2, pp. 581–601, 2021.

[33] T. J. Miao, B. M. Yu, Y. G. Duan, and Q. T. Fang, "A fractal analysis of permeability for fractured rocks," *International Journal of Heat and Mass Transfer*, vol. 81, pp. 75–80, 2015.